COMM. MATH. SCI.
Vol. 4, No. 3, pp. 575–590

PDE'S ON SURFACES – A DIFFUSE INTERFACE APPROACH*

ANDREAS RÄTZ† AND AXEL VOIGT‡

Abstract. We introduce a new approach to deal with the numerical solution of partial differential equations on surfaces. Thereby we reformulate the problem on a larger domain in one higher dimension and introduce a diffuse interface region of a phase-field variable, which is defined in the whole domain. The surface of interest is now only implicitly given by the 1/2-level set of this phase-field variable. Formal matched asymptotics show the convergence of the reformulated problem to the original PDE on the surface, as the diffuse interface width shrinks to zero. The main advantage of the approach is the possibility to formulate the problem on a Cartesian grid. With adaptive grid refinement the additional computational cost resulting from the higher dimension can be significantly reduced. Examples on linear diffusion and nonlinear phase separation demonstrate the wide applicability of the method.

Key words. PDEs on surfaces, implicit surfaces, phase-field approximation, asymptotic analysis, Cahn-Hilliard equation, adaptive finite elements

Subject classifications. 35K55, 35K65, 37E35

1. Introduction

While the solution of PDEs on Cartesian grids has become a standard tool in computational science, numerical approaches to solve PDEs on surfaces is much less understood. However such problems received growing interest over the last years, due to a variety of applications. Problems of interest include image processing (e.g. [15] image the human brain), geometry (e.g. [11] deal with splines on manifolds), physiology (e.g. [10] model the liquid delivery into the lung and analyse the role of surfactants), cell-biology (e.g. [2] study domain formation in vesicles), solidification (e.g. [16] simulate ice formation on aircrafts) and gravitation (e.g. [13] simulate the bending of space and time in the surrounding of black holes).

As long as a triangulation of the surface is available such problems can be solved by parametric finite elements. See Fig. 1.1 for the solution of a viscous Cahn-Hilliard equation on various surfaces. The equations for the concentration u and the chemical potential μ on a surface Γ are given by

$$u_t = \nu \Delta_\Gamma \mu, \tag{1.1}$$

$$\mu = -\gamma \Delta_\Gamma u + \gamma^{-1} G'(u) + \alpha \gamma u_t \tag{1.2}$$

with Δ_Γ the surface Laplacian, $G(u) := 18u^2(1-u^2)$ a double well potential, $\nu > 0$ a constant mobility, $\alpha > 0$ a constant kinetic coefficient and $\gamma > 0$ a small parameter. $u = 0$ and $u = 1$ are the two stable steady states, representing the two phases. As initial conditions we use a small zero mean perturbation of $u = 0.5$.

In a finite element software package as AMDiS [22] the same algorithms as used on a Cartesian grid can be used to solve problems on triangulated surfaces. However,

*Received: November 14, 2005; accepted (in revised version): July 6, 2006. Communicated by Michael Holst.
Financial support is acknowledged by DFG through SPP 1095 (grant Vo 899/3-1) and EU through FP6 (grant NMP-STRP 06447 MagDot).

†Crystal Growth Group, Research Center Caesar, Ludwig-Erhard-Allee 2, 53175 Bonn, Germany (raetz@caesar.de).

‡Crystal Growth Group, Research Center Caesar, Ludwig-Erhard-Allee 2, 53175 Bonn, Germany, and Institut for Pure and Applied Mathematics, University of California, Los Angeles, Los Angeles, CA 90095-7121, USA (voigt@caesar.de).

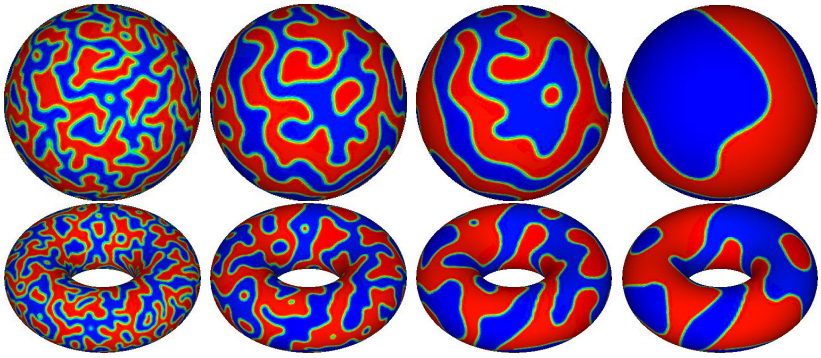

FIG. 1.1. *Coarsening in the viscous Cahn-Hilliard equation. Initial condition* $u=0.5$ *(slightly perturbed), dark denotes* $u=0$ *and light denotes* $u=1$. *(top) Evolution on a sphere at timesteps* $t=1.3\cdot10^{-3}$, $t=4.4\cdot10^{-3}$, $t=1.2\cdot10^{-2}$ *and* $t=1.8\cdot10^{-1}$, *(bottom) evolution on a torus at timesteps* $t=1.4\cdot10^{-3}$, $t=5.4\cdot10^{-3}$, $t=2.0\cdot10^{-2}$ *and* $t=7.4\cdot10^{-2}$. *All simulations are performed in AMDiS [22].*

well known convergence results of the numerical scheme on a Cartesian grid, can not easily be transferred to the algorithm if applied to solve the same PDE on a surface. Some of the resulting numerical analysis problems for elliptic equations are addressed in [12], but a comparable theory for parabolic problems is not available. A second problem with this approach results from the need of an appropriate surface mesh, which might not be easy to generate for complicated surfaces. Furthermore, if the surface evolves by itself, possible topological changes are hard to include in this approach.

To overcome these difficulties there have been several attempts to solve PDEs on only implicitly defined surfaces. In [3] an Eulerian method for this problem has been introduced using only a discretization on a Cartesian grid. By representing a $(d-1)$-dimensional surface as the 0-level set of a level set function ϕ defined in a domain $\Omega\subset\mathbb{R}^d$ containing the surface, one can derive the Eulerian representation by replacing the surface derivatives with projections of the derivatives in the embedding Eulerian space and then solve this new representation on a Cartesian grid. In particular, the surface gradient and surface Laplacian are written as

$$\nabla_\Gamma u = P\nabla\tilde{u} \quad \text{and} \quad \Delta_\Gamma u = \nabla\cdot(P\nabla\tilde{u}), \tag{1.3}$$

with the projection

$$P = I - \frac{\nabla\phi\otimes\nabla\phi}{|\nabla\phi|^2}, \tag{1.4}$$

onto the surface; note that $\nabla\phi$ is normal to Γ. Furthermore it is assumed that $\tilde{u}$ is a smooth function defined in Ω, and u is the restriction of $\tilde{u}$ to the surface. In order to increase the efficiency of the method one can apply a narrow band approach where all operations are performed on a narrow band surrounding the surface. This procedure has been applied to linear diffusion, anisotropic diffusion, and reaction diffusion equations [3], to the Eikonal equation [14] and more recently it has been extended to solve higher order equations [9], on surfaces of varying complexity. The

viscous Cahn-Hilliard equation (1.1), (1.2) in this setting reads

$$\tilde{u}_t = \nu \nabla \cdot (P \nabla \tilde{\mu}), \tag{1.5}$$

$$\tilde{\mu} = -\gamma \nabla \cdot (P \nabla \tilde{u}) + \gamma^{-1} G'(\tilde{u}) + \alpha \gamma \tilde{u}_t. \tag{1.6}$$

The equation has been solved in [9] on the same domains as used in Fig. 1.1, leading to similar results. But despite the wide applicability of the method, several difficulties have been reported. Applying the method to diffusion problems results in a degenerate diffusion equation in the embedding space, as there is no diffusion in the direction perpendicular to the surface. The degeneracy problem is most severe for higher order equations and has been pointed out in [9]. A second difficulty arises by extending off initial data of the surface to the embedding domain. This has to be done with care, because the solution at the surface will be affected by these extensions. However, no matter how the extension is chosen it will change in time, and re-extension might be necessary from time to time. Furthermore the method relies on the signed-distance property of the level set function. All these difficulties can probably be overcome and have been dealt with in the level set context [21, 17]. Recently [8] improved the approach to overcome some of the difficulties. However, with no doubt, it is a powerful approach, which has already been applied to study evolution equations on varying surfaces [23].

We will present a different approach to solve PDEs on implicitly defined surfaces, which is based on a diffuse interface method, where we assume the surface to be represented by the 1/2-level set of a phase-field variable ϕ defined in a domain $\Omega \subset \mathbb{R}^d$ containing the surface Γ. The key ingredient is the function $B = B(\phi) = \phi^2(1-\phi)^2$, which vanishes outside the diffuse interface. Such a mobility function has been introduced in [5] to model surface diffusion within a diffuse interface approximation. Here the function $B(\phi)$ allows us to rewrite rather general quasilinear elliptic and parabolic PDEs on surfaces into PDEs in $\mathbb{R}^d$. The implicit version of the viscous Cahn-Hilliard equation (1.1), (1.2) for example reads

$$B(\phi)\tilde{u}_t = \nu \nabla \cdot ((\delta(\epsilon) + B(\phi)) \nabla \tilde{\mu}), \tag{1.7}$$

$$B(\phi)\tilde{\mu} = -\gamma \nabla \cdot ((\delta(\epsilon) + B(\phi)) \nabla \tilde{u}) + \gamma^{-1} B(\phi) G'(\tilde{u}) + \alpha \gamma B(\phi) \tilde{u}_t \tag{1.8}$$

with $\tilde{u}$ and $\tilde{\mu}$ smooth functions defined in $\Omega \subset \mathbb{R}^d$ approximating the solutions of (1.1), (1.2) at the interface. Furthermore $\epsilon > 0$ measures the width of the diffuse interface and $\delta(\epsilon)$ is chosen such that $0 < \delta(\epsilon) \ll \epsilon$. For the increase of numerical efficiency we use an adaptively refined mesh. In this paper we will analyze the phase-field approach in detail. A similar approach to deal with elliptic PDEs on implicit surfaces has been studied in [4].

The paper is organized as follows. In Section 2 we introduce the diffuse interface approach for a linear diffusion equation, provide a matched asymptotic analysis showing the formal convergence towards the sharp interface problem as the width of the diffuse interface shrinks to zero and compare numerical results of the diffuse interface ansatz with analytic solutions and with numerical results of sharp interface simulations of the diffusion equation. In Section 3 we consider the viscous Cahn-Hilliard equation as an example of a fourth order equation and again show through matched asymptotic analysis the formal convergence of the equations (1.7) and (1.8) to the viscous Cahn-Hilliard equation on a surface (1.1) and (1.2). Furthermore we show the thermodynamic consistency of the formulation. In Section 4 we describe an adaptive finite element discretization of the approximated viscous Cahn-Hilliard equation and

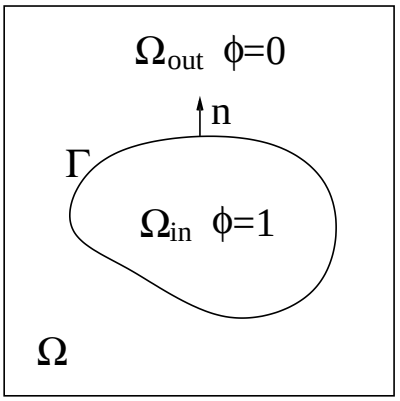

FIG. 2.1. *Schematic picture for* $d=2$.

in Section 5 we show several simulation results for (1.7) and (1.8). Finally we draw conclusions.

2. Diffuse interface approximation

We consider a fixed closed and smooth $(d-1)$-dimensional surface $\Gamma\subset\mathbb{R}^d$ with $d\geq 2$ and are interested in solving PDEs on Γ.

2.1. Linear diffusion equation. To fix ideas we will first consider a linear diffusion equation

$$u_t-\Delta_\Gamma u=f \quad \text{on} \quad \Gamma\times I, \tag{2.1}$$

for $u:\Gamma\times I\to\mathbb{R}$, $I\subset\mathbb{R}$, where Δ_Γ denotes the surface Laplacian on Γ and $f:\Gamma\to\mathbb{R}$ is a smooth function. Furthermore we assume

$$u(x,0)=u_0(x) \quad \text{for} \quad x\in\Gamma$$

for some prescribed and smooth initial solution $u_0:\Gamma\to\mathbb{R}$. Let $\mathbf{n}:\Gamma\to S^{d-1}$ denote a normal to the surface Γ. Assuming that Γ is contained in a bounded domain $\Omega\subset\mathbb{R}^d$ with sufficiently smooth boundary $\partial\Omega$ this defines an interface separating Ω in two domains Ω_{in} and Ω_{out}, where we use the convention that $\mathbf{n}$ points from the inner domain Ω_{in} into the outer domain Ω_{out}. Then one can define an indicator function ϕ_0 being 1 in Ω_{in} and 0 in Ω_{out} (see Fig. 2.1). In order to introduce a diffuse interface approximation of (2.1) we assume that Γ can be approximated by the 1/2-level set Γ_ϵ of a phase-field function $\phi=\phi_\epsilon:\Omega\to\mathbb{R}$ with $\epsilon>0$ obtained by smearing out the discrete function ϕ_0 on a lengthscale of order ϵ. To be more precise we consider a monotone decreasing function $\psi:\mathbb{R}\to(0,1)$ with

$$\lim_{z\to+\infty}\psi(z)=0 \quad \text{and} \quad \lim_{z\to-\infty}\psi(z)=1$$

and

$$\lim_{|z|\to\infty} z\psi(z)^2(1-\psi(z))^2=0.$$

For the signed distance function $r = r(x) : \Omega \to \mathbb{R}$ measuring the distance of a point x to Γ being positive in Ω_{out} and negative in Ω_{in} we define

$$\phi_\epsilon(x) := \psi\left(\frac{r(x)}{\epsilon}\right).$$

This means that ϕ_ϵ is obtained from ϕ_0 by smearing out in the direction normal to Γ. Then a phase-field approximation for (2.1) can be given by

$$B(\phi_\epsilon)\tilde{u}_t - \nabla\cdot(\delta(\epsilon) + B(\phi_\epsilon))\nabla\tilde{u}) = B(\phi_\epsilon)\tilde{f} \quad \text{on} \quad \Omega \tag{2.2}$$

for $\tilde{u} : \Omega \times I \to \mathbb{R}$ with $B(\phi) = \phi^2(1-\phi)^2$ and a sufficiently smooth extension $\tilde{f}$ of f to the domain Ω. Additionally we consider an intitial solution $\tilde{u}_0 : \Omega \to \mathbb{R}$ with $\tilde{u}_0|_\Gamma = u_0$ and assume the initial condition

$$\tilde{u}(x,0) = \tilde{u}_0(x) \quad \text{for} \quad x \in \Omega.$$

Furthermore one has to assume certain boundary conditions for $\tilde{u}$ and $\tilde{u}_0$ on $\partial\Omega$. In all numerical applications presented here we will consider cubic domains Ω and periodic boundary conditions for the solutions.

The addition of the paramteter $\delta = \delta(\epsilon)$ to the function B in the second order term of (2.2) makes the above mathematical problem well posed. For the asymptotic analysis (see section 2.2) to yield the diffusion equation (2.1) as $\epsilon \to 0$ the choice $\delta = \epsilon$ would be sufficient, but in order to obtain satisfactory numerical results a much smaller value has to be required. The dependence of the solution on δ will be studied in Table 2.2. Thus the parameter δ should be viewed as having a regularizing meaning.

2.2. Asymptotic analysis for linear diffusion equation. We now provide a matched asymptotic analysis (see e.g. [18, 5]) to show the formal convergence of (2.2) to (2.1) as $\epsilon \to 0$. In the following we will drop the $\tilde{}$ in the notation, thus u and f now also denote functions in Ω. Furthermore we assume $\delta(\epsilon) = \mathcal{O}(\epsilon)$.

2.2.1. New coordinates. New coordinates are established in a neighborhood of the interface Γ. To this end $r = r(x;\epsilon)$ is defined as the signed distance of x from Γ_ϵ being positive in Ω_{out}. Furthermore let $\mathbf{X} : S \to \mathbb{R}^d$ be a parametric representation of Γ_ϵ, where S is an oriented surface of dimension $d-1$. Let $\mathbf{n} = \mathbf{n}(s;\epsilon)$, $s \in S$, denote the normal. Then we assume that for $0 < \rho \ll 1$ there exists a neighborhood

$$U_\epsilon = \{(x) \in \Omega : |r(x;\epsilon)| < \rho\} \tag{2.3}$$

of Γ_ϵ such that one can write $x = \mathbf{X}(s;\epsilon) + r(x;\epsilon)\mathbf{n}(s;\epsilon)$ for $x \in U_\epsilon$. Now one transforms u and ϕ to the new coordinate system:

$$\begin{aligned}
\hat{u}(r,s,t;\epsilon) &:= u(\mathbf{X}(s;\epsilon) + r\mathbf{n}(s;\epsilon), t;\epsilon), \qquad x \in U_\epsilon,\\
\hat{\phi}(r,s;\epsilon) &:= \phi_\epsilon(\mathbf{X}(s;\epsilon) + r\mathbf{n}(s;\epsilon)) = \psi\left(\frac{r}{\epsilon}\right), \qquad x \in U_\epsilon,\\
\hat{f}(r,s;\epsilon) &:= f(\mathbf{X}(s;\epsilon) + r\mathbf{n}(s;\epsilon)), \qquad x \in U_\epsilon.
\end{aligned}$$

Furthermore a stretched variable is introduced $z := \frac{r}{\epsilon}$, and one defines

$$\begin{aligned}
U(z,s,t;\epsilon) &:= \hat{u}(r,s,t;\epsilon),\\
\Phi(z,s;\epsilon) &:= \hat{\phi}(r,s;\epsilon) = \psi(z),\\
F(z,s;\epsilon) &:= \hat{f}(r,s;\epsilon).
\end{aligned}$$

In addition the following Taylor expansion approximations for small ϵ are assumed to be valid

$$u(x,t;\epsilon) = u_0(x,t) + \mathcal{O}(\epsilon), \tag{2.4}$$
$$\hat{u}(r,s,t;\epsilon) = \hat{u}_0(r,s,t) + \mathcal{O}(\epsilon), \tag{2.5}$$
$$U(z,s,t;\epsilon) = U_0(z,s,t) + \epsilon U_1(z,s,t) + \epsilon^2 U_2(z,s,t) + \mathcal{O}(\epsilon^3), \tag{2.6}$$
$$f(x) = f_0(x), \tag{2.7}$$
$$\hat{f}(r,s;\epsilon) = \hat{f}_0(r,s) + \mathcal{O}(\epsilon), \tag{2.8}$$
$$F(z,s;\epsilon) = F_0(z,s) + \mathcal{O}(\epsilon), \tag{2.9}$$
$$\phi_\epsilon(x) = \phi_0(x) + \mathcal{O}(\epsilon), \tag{2.10}$$
$$\hat{\phi}(r,s;\epsilon) = \hat{\phi}_0(r,s) + \mathcal{O}(\epsilon), \tag{2.11}$$
$$\Phi(z,s;\epsilon) = \Phi_0(z,s) = \psi(z), \tag{2.12}$$

for which (2.4), (2.5) and (2.10), (2.11) are called outer expansions while (2.6), (2.12) are called inner expansion. It is assumed that these hold simultaneously in some overlapping region and represent the same functions, which yields the matching conditions

$$\lim_{r\to\pm 0} \hat{u}_0(r,s,t) = \lim_{z\to\pm\infty} U_0(z,s,t), \tag{2.13}$$
$$\lim_{r\to\pm 0} \hat{\phi}_0(r,s) = \lim_{z\to\pm\infty} \Phi_0(z,s). \tag{2.14}$$

Let $H = H(s;\epsilon) = \sum_i^{d-1} \kappa_i$ denote the mean curvature of Γ with the principal curvatures κ_i. The transform of the derivatives into the new coordinates (z,s) lead

$$\nabla u = \epsilon^{-1} \partial_z U \mathbf{n} + \sum_{i,j=1}^{2} g^{ij} \partial_{s_i} U \partial_{s_j} \mathbf{X} + \mathcal{O}(\epsilon), \tag{2.15}$$
$$\Delta u = \epsilon^{-2} \partial_z^2 U + \epsilon^{-1} H \partial_z U + \Delta_\Gamma U + \mathcal{O}(\epsilon), \tag{2.16}$$

where $g_{ij} := \phi_{s_i} \cdot \phi_{s_j}$ and $(g^{ij}) := (g_{ij})^{-1}$. We will need the formula

$$\begin{aligned} &\nabla \cdot ((\delta(\epsilon) + B(\phi)) \nabla u) \\ &\quad = \epsilon^{-2} \partial_z ((\delta(\epsilon) + B(\Phi)) \partial_z U) + \epsilon^{-1} (\delta(\epsilon) + B(\Phi)) H \partial_z U + B(\Phi) \Delta_\Gamma U + \mathcal{O}(\epsilon). \end{aligned} \tag{2.17}$$

Because the surface Γ is fixed, we have the time derivative

$$\partial_t u = \partial_t U.$$

2.2.2. Outer expansion. By assumption we have $\phi_0 = 1$ in Ω_{in} and $\phi_0 = 0$ in Ω_{out} and therefore $\lim_{z\to+\infty} \Phi_0 = \lim_{r\to+0} \phi_0 = 0$ as well as $\lim_{z\to-\infty} \Phi_0 = \lim_{r\to-0} \phi_0 = 1$.

2.2.3. Inner expansion. Using (2.17) in (2.2) we obtain in $\mathcal{O}(\epsilon^{-2})$

$$\partial_z (B(\Phi_0) \partial_z U_0) = 0$$

which yields $\partial_z U_0 = 0$. From this one gets in $\mathcal{O}(\epsilon^{-1})$

$$\partial_z (B(\Phi_0) \partial_z U_1) = 0$$

and therefore $\partial_z U_1 = 0$. And finally we have in $\mathcal{O}(\epsilon^0)$

$$B(\Phi_0)\partial_t U_0 - \partial_z(B(\Phi_0)\partial_z U_2) - B(\Phi_0)\Delta_\Gamma U_0 = B(\Phi_0)F_0, \tag{2.18}$$

where we have used $\partial_{s_i}\Phi_0 = 0$ for $i = 1,2$. Furthermore one easily verifies that $\partial_z F_0 = 0$, and integration of (2.18) yields

$$\int_{-\infty}^{+\infty} B(\Phi_0)\,\mathrm{d}z\partial_t U_0 - \int_{-\infty}^{+\infty} B(\Phi_0)\,\mathrm{d}z\Delta_\Gamma U_0 = \int_{-\infty}^{+\infty} B(\Phi_0)\,\mathrm{d}z F_0.$$

Dividing this equation by $\int_{-\infty}^{+\infty} B(\Phi_0)\,\mathrm{d}z$ we end up with

$$\partial_t U_0 - \Delta_\Gamma U_0 = F_0.$$

Thus with $F_0 = f$ and $\lim_{z\to\pm\infty} U_0 = \lim_{r\to\pm 0} u_0 = u_0|_\Gamma$ we have shown the formal convergence to the linear diffusion equation (2.1) on the surface Γ.

To provide a rigorous proof of this formally derived result one would have to apply the techniques of [1].

2.3. Numerical results. As an example we consider the sphere $\Gamma = S^2$, which is embedded into the domain $\Omega = (-2,2)^3$. The function

$$\phi_\epsilon = \phi_\epsilon(x) = \frac{1}{2}\left(1 - \tanh\left(\frac{3}{\epsilon}(|x|-1)\right)\right) = \frac{1}{2}\left(1 - \tanh\left(\frac{3r}{\epsilon}\right)\right) \tag{2.19}$$

serves as a phase-field approximation of Γ. On $\partial\Omega$ we assume periodic boundary conditions for $\tilde{u}$. For the heat equation (2.1) and (2.2), respectively, we take the right hand side function

$$f(x) = 2x_1 \quad \text{for} \quad x \in S^2 \quad \text{and} \quad \tilde{f}(x) = 2x_1 \quad \text{for} \quad x \in \Omega,$$

which yields the spherical harmonic

$$u(x) = x_1 \tag{2.20}$$

as the stationary solution of (2.1) and therefore a numerical benchmark to test our approach on.

Fig. 2.2 shows the solution of (2.1) and (2.2) with initial functions $u(x,0) = \tilde{u}(x,0) = 0$. Different timesteps are depicted until the stationary solution is reached.

The dynamic evolution in both approaches nicely agrees and both simulations converge to the stationary solution of (2.1) and (2.2), respectively. The solutions of

$$-\Delta_\Gamma u = f \tag{2.21}$$

and

$$-\nabla\cdot((\delta(\epsilon) + B(\phi_\epsilon))\nabla\tilde{u}) = B(\phi_\epsilon)\tilde{f} \tag{2.22}$$

are shown in Fig. 2.3. The stationary solution in both approaches can not be distinguished from each other and agree with the solution of the dynamic problem at $t = 3.5$. In both cases we have used the parameters $\epsilon = 0.1$ and $\delta = 10^{-5}$.

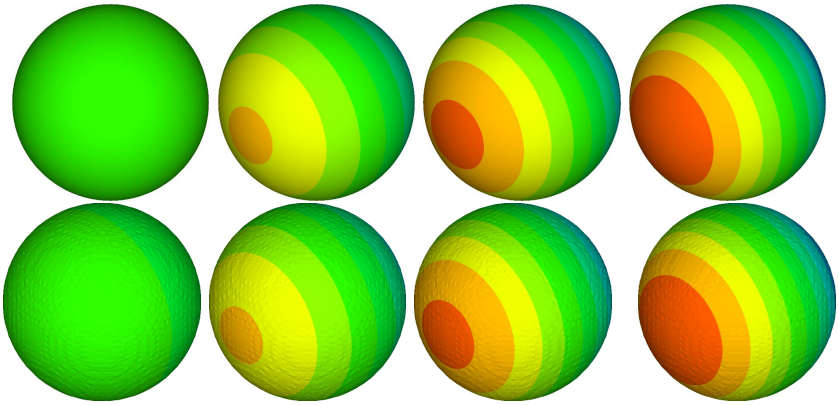

FIG. 2.2. *Evolution of the temperature: (top) solution u of (2.1), (bottom) solution $\tilde{u}|_\Gamma$ of (2.2), both at timesteps $t=0$, $t=0.5$, $t=1.0$ and $t=3.5$.*

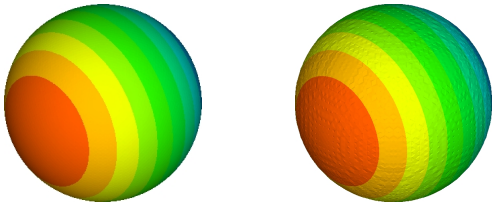

FIG. 2.3. *Stationary temperature: (left) solution u of (2.21), (right) solution $\tilde{u}|_\Gamma$ of (2.22).*

In the following we consider the error of the discrete solution u_h in the L^∞-norm with h being the grid size

$$\|u-u_h\|_{L^\infty(\Gamma)}, \tag{2.23}$$

where u denotes the analytic solution (2.20). The grid size h is represented by the number of grid points in the interface region $p\in\mathbb{N}$. Table 2.1 shows the convergence of the discrete solution towards the analytic one as $\epsilon,h\to 0$ with fixed $\delta=10^{-6}$. In Table 2.2 one can see for fixed $\epsilon=0.3$ the approximation of the analytic solution with decreasing δ.

	$p=2$	$p=3$	$p=4$	$p=5$	$p=6$
$\epsilon=0.5$	$3.35\cdot10^{-2}$	$3.06\cdot10^{-2}$	$2.50\cdot10^{-2}$	$2.62\cdot10^{-2}$	$2.63\cdot10^{-2}$
$\epsilon=0.4$	$2.92\cdot10^{-2}$	$1.93\cdot10^{-2}$	$1.85\cdot10^{-2}$	$1.76\cdot10^{-2}$	$1.64\cdot10^{-2}$
$\epsilon=0.3$	$3.15\cdot10^{-2}$	$1.52\cdot10^{-2}$	$1.21\cdot10^{-2}$	$9.65\cdot10^{-3}$	$9.28\cdot10^{-3}$
$\epsilon=0.2$	$1.97\cdot10^{-2}$	$7.59\cdot10^{-3}$	$5.81\cdot10^{-3}$	$4.90\cdot10^{-3}$	$3.93\cdot10^{-3}$
$\epsilon=0.1$	$9.58\cdot10^{-3}$	$2.80\cdot10^{-3}$	$1.89\cdot10^{-3}$	$1.07\cdot10^{-3}$	$6.26\cdot10^{-4}$

TABLE 2.1. *Error in the L^∞-norm with fixed $\delta=10^{-6}$*

.

	$p=2$	$p=3$	$p=4$	$p=5$	$p=6$
$\delta=10^{-2}$	$6.49\cdot10^{-1}$	$6.79\cdot10^{-1}$	$6.86\cdot10^{-1}$	$6.90\cdot10^{-1}$	$6.93\cdot10^{-1}$
$\delta=10^{-3}$	$1.73\cdot10^{-1}$	$1.86\cdot10^{-1}$	$1.90\cdot10^{-1}$	$1.92\cdot10^{-1}$	$1.94\cdot10^{-1}$
$\delta=10^{-4}$	$3.31\cdot10^{-2}$	$2.69\cdot10^{-2}$	$2.04\cdot10^{-2}$	$1.92\cdot10^{-2}$	$1.89\cdot10^{-2}$
$\delta=10^{-5}$	$2.92\cdot10^{-2}$	$1.26\cdot10^{-3}$	$9.46\cdot10^{-3}$	$7.34\cdot10^{-3}$	$6.58\cdot10^{-3}$
$\delta=10^{-6}$	$3.15\cdot10^{-2}$	$1.52\cdot10^{-2}$	$1.21\cdot10^{-2}$	$9.65\cdot10^{-3}$	$9.28\cdot10^{-3}$

TABLE 2.2. *Error in the L^∞-norm with fixed $\epsilon=0.3$*

.

Both tables indicate that within the constraint of limited computing time and memory the choice $\delta=10^{-5}$, $\epsilon=0.1$ and $p=5$ leads to acceptable tolerances. These parameters will be used in the more demanding computations in section 5.

Furthermore we would like to mention that changing the extension $\tilde{f}$ in the linear diffusion equation (2.2) in the numerical studies into $\tilde{f}(x)=\frac{2x_1}{|x|^2}$ for $x\neq0$ and $\tilde{f}(0)=0$ yields that the influence of the choice of the extension of parameters is negligible.

2.4. More general parabolic equations. After this promising result we want to generalize the equation and summerize the ingredients for the diffuse-interface approach to solve problems on surfaces. Denoting the tangent space of Γ in $x\in\Gamma$ with $T_x\Gamma$ a more general second order PDE on a surface Γ reads

$$u_t-\nabla_\Gamma\cdot(A\nabla_\Gamma u)+b\cdot\nabla_\Gamma u+cu=f$$

with a positive definite symmetric endomorphism $A=A(u,\nabla_\Gamma u,x,t):T_x\Gamma\to T_x\Gamma$, $b=b(u,\nabla_\Gamma u,x,t):T_x\Gamma\to\mathbb{R}$, $c=c(u,\nabla_\Gamma u,x,t)\in\mathbb{R}$ and $f=f(x,t)$. Here $A(\cdot)$, $b(\cdot)$, $c(\cdot)$ and $f(\cdot)$ are assumed to be sufficiently smooth. To transform it into a PDE in Ω we need to extend all parameters in a sufficiently smooth manner. The diffuse interface approximation then reads

$$B(\phi_\epsilon)\tilde{u}_t-\nabla\cdot((\delta(\epsilon)+B(\phi_\epsilon))\tilde{A}\nabla\tilde{u})+B(\phi_\epsilon)\tilde{b}\cdot\nabla\tilde{u}+B(\phi_\epsilon)\tilde{c}\tilde{u}=B(\phi_\epsilon)\tilde{f},$$

where $\tilde{A}$ is a positive definite extension of the endomorphism A to normal vectors and the extension $\tilde{b}$ of b to normal vectors can be arbitrarily chosen. The matched asymptotic analysis can be done along the same lines as for the linear problem.

3. The viscous Cahn-Hilliard equation

We will now return to the viscous Cahn-Hilliard equation (1.1), (1.2) on a closed surface Γ and its diffuse interface approximation on a domain Ω containing the surface

$$B(\phi)u_t=\nu\nabla\cdot((\delta(\epsilon)+B(\phi))\nabla\mu), \tag{3.1}$$

$$B(\phi)\mu=-\gamma\nabla\cdot((\delta(\epsilon)+B(\phi))\nabla u)+\gamma^{-1}B(\phi)G'(u)+\alpha\gamma B(\phi)u_t, \tag{3.2}$$

where we have dropped the subscript ϵ and used ϕ instead of ϕ_ϵ. Besides we have dropped the $\tilde{}$ for u. One has to assume $u(x,0)=u_0(x)$ for $x\in\Omega$ and an initial function $u_0:\Omega\to\mathbb{R}$ coinciding on Γ with the initial function for the sharp interface problem. Furthermore we again assume periodic boundary conditions on $\partial\Omega$.

In the case of a (viscous) Cahn-Hilliard equation in $\mathbb{R}^n$ existence results are known (see e.g. [7]) also with a degenerate mobility function [6]. To the authors' knowledge there are no corresponding results for a Cahn-Hilliard equation on a surface or in the implicit form (3.1), (3.2).

3.1. Thermodynamic consistency. The diffuse-interface approximation to the viscous Cahn-Hilliard equation on a surface (3.1) and (3.2) has the properties of a gradient flow of the following energy

$$E(u) = \int_\Omega \gamma^{-1} B(\phi) G(u) + \gamma \frac{1}{2} (\delta(\epsilon) + B(\phi)) |\nabla u|^2. \tag{3.3}$$

The time derivative can thus be computed as

$$\begin{aligned}
\partial_t E(u) &= \int_\Omega \gamma^{-1} B(\phi) G'(u) \partial_t u + \gamma (\delta(\epsilon) + B(\phi)) \nabla u \cdot \nabla u_t \\
&= \int_\Omega \left(\gamma^{-1} B(\phi) G'(u) - \gamma \nabla \cdot ((\delta(\epsilon) + B(\phi)) \nabla u) \right) u_t \\
&= \int_\Omega (B(\phi)\mu - \alpha\gamma B(\phi) u_t) u_t \\
&= \int_\Omega \mu\nu \nabla \cdot ((\delta(\epsilon) + B(\phi)) \nabla \mu) - \alpha\gamma B(\phi) (u_t)^2 \\
&= \int_\Omega -\nu (\delta(\epsilon) + B(\phi)) (\nabla \mu)^2 - \alpha\gamma B(\phi) (u_t)^2 \leq 0,
\end{aligned}$$

where eq. (1.7) and (1.8) have been used. Thus the dissipation inequality holds for the introduced diffuse interface approximation, which shows its thermodynamic consistency. The same holds for the two limiting cases:
(A) the Cahn-Hilliard equation, which is obtained as $\alpha \to 0$

$$\begin{aligned}
B(\phi) u_t &= \nu \nabla \cdot ((\delta(\epsilon) + B(\phi)) \nabla \mu), \\
B(\phi) \mu &= -\gamma \nabla \cdot ((\delta(\epsilon) + B(\phi)) \nabla u) + \gamma^{-1} B(\phi) G'(u),
\end{aligned}$$

and
(B) the Allen-Cahn equation, which can be obtained as $\nu \to \infty$

$$\alpha\gamma B(\phi) u_t = \gamma \nabla \cdot ((\delta(\epsilon) + B(\phi)) \nabla u) - \gamma^{-1} B(\phi) G'(u).$$

It remains to show the convergence of the diffuse interface approximation to the viscous Cahn-Hilliard equation on a surface (1.1) and (1.2) as $\epsilon \to 0$.

3.2. Asymptotic analysis for viscous Cahn-Hilliard equation. Note that we have two distinguished interface parameters: γ the intrinsic diffuse interface width in the viscous Cahn-Hilliard equation on the surface Γ, and ϵ the diffuse interface width of the phase-field approximation in Ω. Here we consider the limit $\epsilon \to 0$.

3.2.1. New coordinates. Extending the notation in Section 2.2 by introducing

$$\hat{\mu}(r,s,t;\epsilon) := \mu(\mathbf{X}(s;\epsilon) + r\mathbf{n}(s;\epsilon), t; \epsilon), \qquad x \in U_\epsilon$$

and

$$M(z,s,t;\epsilon) := \hat{\mu}(r,s,t;\epsilon)$$

and assuming the Taylor expansion approximations for small ϵ to be valid

$$\mu(x,t;\epsilon) = \mu_0(x,t) + \mathcal{O}(\epsilon), \tag{3.4}$$

$$\hat{\mu}(r,s,t;\epsilon) = \hat{\mu}_0(r,s,t) + \mathcal{O}(\epsilon), \tag{3.5}$$

$$M(z,s,t;\epsilon) = M_0(z,s,t) + \epsilon M_1(z,s,t) + \epsilon^2 M_2(z,s,t) + \mathcal{O}(\epsilon^3) \tag{3.6}$$

and that these hold simultaneously in some overlapping region and represent the same functions, we obtain the additional matching condition

$$\lim_{r\to\pm 0}\hat{\mu}_0(r,s,t)=\lim_{z\to\pm\infty}M_0(z,s,t). \tag{3.7}$$

3.2.2. Outer expansion. See the case of the linear diffusion equation.

3.2.3. Inner expansion. Using the inner expansions in (3.1) and (3.2) we obtain in
$\mathcal{O}(\epsilon^{-2})$

$$\begin{aligned}\partial_z(B(\Phi_0)\partial_z M_0)&=0,\\ \partial_z(B(\Phi_0)\partial_z U_0)&=0\end{aligned}$$

which yield $\partial_z M_0=0$ and $\partial_z U_0=0$. From these one gets in
$\mathcal{O}(\epsilon^{-1})$

$$\begin{aligned}\partial_z(B(\Phi_0)\partial_z M_1)&=0,\\ \partial_z(B(\Phi_0)\partial_z U_1)&=0\end{aligned}$$

and therefore $\partial_z M_1=0$ and $\partial_z U_1=0$. And finally we have in
$\mathcal{O}(\epsilon^{0})$

$$\begin{aligned}B(\Phi_0)\partial_t U_0&=\nu(\partial_z(B(\Phi_0)\partial_z M_2)+B(\Phi_0)\Delta_\Gamma M_0),\\ B(\Phi_0)M_0&=-\gamma\big(\partial_z(B(\Phi_0)\partial_z U_2)+B(\Phi_0)\Delta_\Gamma U_0\big)\\ &\quad+\gamma^{-1}B(\Phi_0)G'(U_0)+\alpha\gamma B(\Phi_0)\partial_t U_0\end{aligned}$$

Integration of both equations yields

$$\begin{aligned}\int_{-\infty}^{+\infty}B(\Phi_0)\,\mathrm{d}z\partial_t U_0&=\nu\int_{-\infty}^{+\infty}B(\Phi_0)\,\mathrm{d}z\Delta_\Gamma M_0,\\ \int_{-\infty}^{+\infty}B(\Phi_0)\,\mathrm{d}z M_0&=-\int_{-\infty}^{+\infty}B(\Phi_0)\,\mathrm{d}z\gamma\Delta_\Gamma U_0\\ &\quad+\int_{-\infty}^{+\infty}B(\Phi_0)\,\mathrm{d}z\gamma^{-1}G'(U_0)+\int_{-\infty}^{+\infty}B(\Phi_0)\,\mathrm{d}z\alpha\gamma\partial_t U_0.\end{aligned}$$

Dividing these equations by $\int_{-\infty}^{+\infty}B(\Phi_0)\,\mathrm{d}z$ we end up with

$$\begin{aligned}\partial_t U_0&=\nu\Delta_\Gamma M_0,\\ M_0&=-\gamma\Delta_\Gamma U_0+\gamma^{-1}G'(U_0)+\alpha\gamma\partial_t U_0,\end{aligned}$$

on Γ, which is by matching conditions (2.13) and (3.7) the viscous Cahn-Hilliard equation (1.1) and (1.2) for $u_0|_\Gamma$ and $\mu_0|_\Gamma$.

4. Numerical approach

We adapt the numerical approach used in [19] to solve a viscous Cahn-Hilliard equation with a degenerate mobility function. Furthermore we use the definition

$$C(\phi):=\delta(\epsilon)+B(\phi).$$

4.1. Finite element discretization. The time interval is split by discrete time instants $0=t_0<t_1<\ldots$, from which one gets the time steps $\Delta t_m := t_{m+1}-t_m$. The derivative of the doublewell potential is linearized by

$$\begin{aligned} G'(u^{(m+1)}) &\approx G'(u^{(m)}) + G''(u^{(m)})(u^{(m+1)}-u^{(m)}) \\ &= G''(u^{(m)})u^{(m+1)} + G'(u^{(m)}) - G''(u^{(m)})u^{(m)}. \end{aligned}$$

Using this time discretization one ends up with the weak formulation

$$\begin{aligned} &\frac{1}{\Delta t_m}\int_\Omega B(\phi)u^{(m+1)}\psi + \nu\int_\Omega C(\phi)\nabla\mu^{(m+1)}\cdot\nabla\psi \\ &\quad = \frac{1}{\Delta t_m}\int_\Omega B(\phi)u^{(m)}\psi, \\ &-\int_\Omega B(\phi)\mu^{(m+1)}\psi + \gamma\int_\Omega C(\phi)\nabla u^{(m+1)}\cdot\nabla\psi \\ &\qquad + \gamma^{-1}\int_\Omega B(\phi)G''(u^{(m)})u^{(m+1)}\psi + \frac{\gamma\alpha}{\Delta t_m}\int_\Omega B(\phi)u^{(m+1)}\psi \\ &\quad = \frac{\gamma\alpha}{\Delta t_m}\int_\Omega B(\phi)u^{(m)}\psi - \gamma^{-1}\int_\Omega B(\phi)(G'(u^{(m)}) - G''(u^{(m)})u^{(m)})\psi \end{aligned}$$

for all $\psi\in X^d := \{\psi\in H^1(\Omega) : \psi_{|\partial\Omega} \text{ periodic}\}$. To discretize in space, let $\mathcal{T}_h$ be a conforming triangulation of Ω. Define the finite element space of globally continuous, piecewise linear elements $\mathbb{V}_h = \{v_h\in X^d : v_h|_T\in\mathbb{P}^1\ \forall T\in\mathcal{T}_h\}$. The space discretization now reads: Find $u_h^{(m+1)}, \mu_h^{(m+1)}\in\mathbb{V}_h$ such that

$$\begin{aligned} &\frac{1}{\Delta t_m}\int_\Omega B(\phi)u_h^{(m+1)}\psi + \nu\int_\Omega C(\phi)\nabla\mu_h^{(m+1)}\cdot\nabla\psi \\ &\quad = \frac{1}{\Delta t_m}\int_\Omega B(\phi)u_h^{(m)}\psi, \\ &-\int_\Omega B(\phi)\mu_h^{(m+1)}\psi + \gamma\int_\Omega C(\phi)\nabla u_h^{(m+1)}\cdot\nabla\psi \\ &\qquad + \gamma^{-1}\int_\Omega B(\phi)G''(u_h^{(m)})u_h^{(m+1)}\psi + \frac{\gamma\alpha}{\Delta t_m}\int_\Omega B(\phi)u_h^{(m+1)}\psi \\ &\quad = \frac{\gamma\alpha}{\Delta t_m}\int_\Omega B(\phi)u_h^{(m)}\psi - \gamma^{-1}\int_\Omega B(\phi)(G'(u_h^{(m)}) - G''(u_h^{(m)})u_h^{(m)})\psi \end{aligned}$$

for all $\psi\in\mathbb{V}_h$. These lead to a linear system of equations for $U^{(m+1)}$ and $W^{(m+1)}$, with $u_h^{(m+1)} = \sum U_i^{(m+1)}\psi_i$ and $\mu_h^{(m+1)} = \sum W_i^{(m+1)}\psi_i$

$$\begin{aligned} \frac{1}{\Delta t_m}\boldsymbol{M}U^{(m+1)} + \nu\boldsymbol{A}W^{(m+1)} &= \frac{1}{\Delta t_m}\boldsymbol{M}U^{(m)}, \\ -\boldsymbol{M}W^{(m+1)} + \gamma\boldsymbol{A}U^{(m+1)} + \gamma^{-1}\boldsymbol{G}^{\mathrm{i}}U^{(m+1)} + \frac{\gamma\alpha}{\Delta t_m}\boldsymbol{M}U^{(m+1)} &= \frac{\gamma\alpha}{\Delta t_m}\boldsymbol{M}U^{(m)} \\ &\quad -\gamma^{-1}\boldsymbol{G}^{\mathrm{e}} \end{aligned}$$

with

$$\begin{aligned} \boldsymbol{M} &= (M_{ij})M_{ij} = (B(\phi)\psi_i,\psi_j)_\Omega, \\ \boldsymbol{A} &= (A_{ij})A_{ij} = (C(\phi)\nabla\psi_i,\nabla\psi_j)_\Omega, \\ \boldsymbol{G}^{\mathrm{i}} &= (G_{ij}^{\mathrm{i}})G_{ij}^{\mathrm{i}} = (B(\phi)G''(u_h^{(m)})\psi_i,\psi_j)_\Omega, \\ \boldsymbol{G}^{\mathrm{e}} &= (G_i^{\mathrm{e}})G_i^{\mathrm{e}} = (B(\phi)(G'(u_h^{(m)}) - G''(u_h^{(m)}))u_h^{(m)},\psi_i)_\Omega, \end{aligned}$$

where $(\cdot,\cdot)_\Omega$ denotes the L^2 scalar product. Thus, written in block-matrix-form the linear system

$$\begin{pmatrix} \nu\boldsymbol{A} & \frac{1}{\Delta t_m}\boldsymbol{M} \\ -\boldsymbol{M} & \gamma\boldsymbol{A}+\gamma^{-1}\boldsymbol{G}^{\mathrm{i}}+\frac{\gamma\alpha}{\Delta t_m}\boldsymbol{M} \end{pmatrix} \begin{pmatrix} W^{(m+1)} \\ U^{(m+1)} \end{pmatrix} = \begin{pmatrix} \frac{1}{\Delta t_m}\boldsymbol{M}U^{(m)} \\ \frac{\gamma\alpha}{\Delta t_m}\boldsymbol{M}U^{(m)}+\gamma^{-1}\boldsymbol{G}^{\mathrm{e}} \end{pmatrix}$$

has to be solved in every timestep. The system is not symmetric and is iteratively solved by a stabilized bi-conjugate gradient method (BiCGStab). In order to verify the regularity of the system matrix on the left hand side of the above system we assume that (W,U) is a solution of the homogeneous linear system. We denote the corresponding functions in $\mathbb{V}_h$ by μ_h and u_h. Then we arrive at the homogeneous system

$$\frac{1}{\Delta t_m}\int_\Omega B(\phi)u_h\psi+\nu\int_\Omega C(\phi)\nabla\mu_h\cdot\nabla\psi=0, \tag{4.1}$$

$$\begin{aligned} -\int_\Omega B(\phi)\mu_h\psi+\gamma\int_\Omega C(\phi)\nabla u_h\cdot\nabla\psi \\ +\gamma^{-1}\int_\Omega B(\phi)G''(u_h)u_h\psi+\frac{\gamma\alpha}{\Delta t_m}\int_\Omega B(\phi)u_h\psi=0 \end{aligned} \tag{4.2}$$

for all $\psi\in\mathbb{V}_h$. Then we obtain by testing (4.1) equation with μ_h

$$\frac{1}{\Delta t_m}(B(\phi)u_h,\mu_h)_\Omega+\nu(C(\phi)\nabla\mu_h,\nabla\mu_h)_\Omega=0$$

and therefore

$$(B(\phi)u_h,\mu_h)_\Omega\le 0. \tag{4.3}$$

Now we test (4.2) with u_h and arrive at

$$\begin{aligned} -(B(\phi)u_h,\mu_h)_\Omega+\frac{\alpha\gamma}{\Delta t_m}(B(\phi)u_h,u_h)_\Omega \\ +\gamma(C(\phi)\nabla u_h,\nabla u_h)_\Omega+\gamma^{-1}(B(\phi)G''(u_h),u_h)_\Omega=0. \end{aligned}$$

Using (4.3) and

$$(C(\phi)\nabla u_h,\nabla u_h)_\Omega\ge 0$$

one gets with $\|u_h\|_\Omega:=\sqrt{(u_h,u_h)_\Omega}$

$$\frac{\alpha\gamma\delta}{\Delta t_m}\|u_h\|_\Omega^2\le\gamma^{-1}|\Omega|^{1/2}\max(B)\max(|G''|)\,\|u_h\|_\Omega.$$

If we choose Δt_m sufficiently small we obtain $\|u_h\|_\Omega=0$ and therefore $u_h=\mu_h=0$ showing the regularity of the system matrix in the above linear system.

4.2. Adaptivity. Adaptive mesh refinement is a key ingredient to an efficient algorithm for this class of problems, because it helps to reduce the amount of additional work the extra dimension requires. Outside the diffuse interface region the mesh can be rather coarse, without influencing the solution on the surface. As a first approach towards an adaptive scheme we therefore choose a jump residual as an

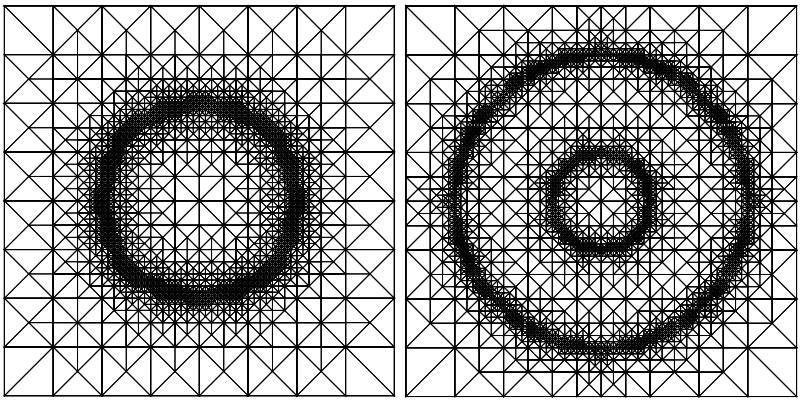

FIG. 4.1. *Adaptively refined mesh (cross section): (left) sphere, (right) torus.*

indicator, to refine the mesh. An error estimate for the viscous Cahn-Hilliard equation itself, accounting for different grid refinements within the diffuse interface, has not been used yet. Thus the grid is homogeneous within the diffuse interface, with approximately $p=5$ grid points in the interface region, which corresponds to $h\approx 0.04$. Fig. 4.1 shows the grid used in the computations.

Furthermore a simple strategy of time adaptivity is used, where the timestep is inversely proportional to the maximum of the normal velocity of the Cahn-Hilliard interface leading to timesteps $\Delta t_m \in [10^{-5}, 10^{-4}]$. This means that the timesteps are increased by approximately one order of magnitude compared to a restriction of order $h^4 \approx 2.56 \cdot 10^{-6}$ an explicit scheme would require.

5. Simulation results

The method is implemented in AMDiS [22]. As in the simulations shown in Fig. 1.1 we use as initial conditions a small zero mean perturbation of $u=0.5$. Again the sphere is given as the level set $\phi=1/2$ of the function (2.19), and in the case of the torus we have used a slightly more complicated tanh-construction than for the sphere. Fig. 5.1 shows the evolution of the diffuse interface approximation of the viscous Cahn-Hilliard equation on a surface. The figure shows the value of u on the $1/2$-level set of the phase-field variable ϕ. The simulation results agree very well with the results shown in Fig. 1.1 at corresponding timesteps, where in all cases we have used the parameters $\gamma=0.05$ and $\alpha=\nu=1.0$ and for the diffuse interface approach $\epsilon=0.1$ and $\delta=10^{-5}$.

The phase-field variable ϕ is in both cases constructed by hand. For more complex geometries this is unfeasible. In these cases an indicator function $I(x)$, with $I(x)=0$ on one side of the surface Γ and $I(x)=1$ on the other side, can be used as an initial function for ϕ. To construct an appropriate phase-field variable to represent the surface, a few time steps of

$$\begin{aligned} \phi_t &= \epsilon^{-1}\nabla\cdot((\delta(\epsilon)+B(\phi))\nabla\mu), \\ \mu &= -\epsilon\Delta\phi+\epsilon^{-1}G'(\phi) \end{aligned}$$

can be performed. The equation will smear out the initial function at the beginning, without changing the $1/2$-level set too much.

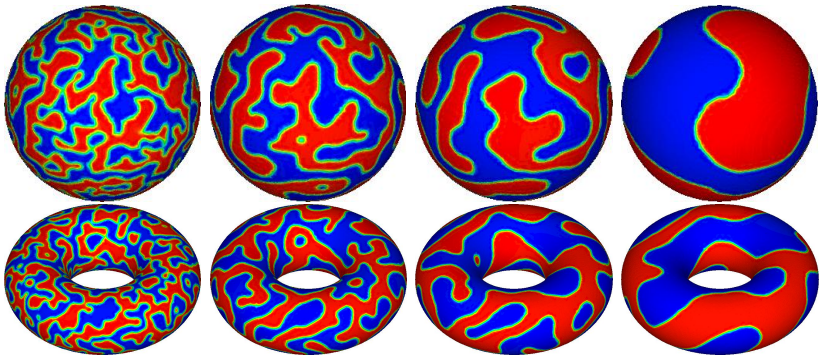

FIG. 5.1. *Coarsening in the viscous Cahn-Hilliard equation (diffuse interface approximation). Dark denotes* $u=0$ *and light denotes* $u=1$. *(top) Evolution on a sphere at timesteps* $t=1.3\cdot10^{-3}$, $t=4.4\cdot10^{-3}$, $t=1.2\cdot10^{-2}$ *and* $t=1.8\cdot10^{-1}$, *(bottom) evolution on a torus at timesteps* $t=1.4\cdot10^{-3}$, $t=5.4\cdot10^{-3}$, $t=2.0\cdot10^{-2}$ *and* $t=7.4\cdot10^{-2}$.

6. Conclusion

We have presented a new approach to solve PDEs on surfaces. The problem is reformulated on a larger domain in one higher dimension and is based on a diffuse interface approximation. The surface is the 1/2-level set of a phase-field variable. Formal matched asymptotics show the convergence to the PDE on the surface as the diffuse interface width shrinks to zero. The method is applied to a linear diffusion problem, which serves as a benchmark and to a nonlinear fourth-order problem to demonstrate its applicability for a general class of PDEs. The approach is here restricted to stationary surfaces, however the way to include motion of the surface is straight forward and is under investigation [20]. The introduced diffuse interface approach has the same advantages as the level set method to solve an Eulerian representation of the PDE on the surface. Especially with the use of an adaptive grid, it can compete with the common narrow-band approach in the level set method. Furthermore, due to the decoupling of the surface representation through the phase-field variable ϕ and the evolution equation, the method is much more insensitive on the way data are extended away from the surface, and the initial properties of ϕ remain unchanged throughout the simulation.

Acknowledgment. We would like to thank Martin Burger and John Lowengrub for stimulating discussions.

REFERENCES

[1] N. D. Alikakos, P. W. Bates and X. Chen, *The convergence of solutions of the Cahn–Hilliard equation to the solution of the Hele–Shaw model*, Arch. Rational Mech. Anal., 128(2), 165-205, 1994.

[2] G. S. Ayton, J. L. McWhirter, P. McMurty and G. A. Voth., *Coupling field theory with continuum mechanics: A simulation of domain formation in giant unilamellar vesicles*, Biophys. J., 88, 3855-3869, 2005.

[3] M. Bertalmio, L.-T. Cheng, S. Osher and G. Sapiro, *Variational problems and partial differential equations on implicit surfaces*, J. Comput. Phys., 174(2), 759-780, 2001.

[4] M. Burger, *Finite element approximation of elliptic partial differential equations on implicit surfaces*, Comput. Vis. Sci., to appear.

[5] J. Cahn, C. M. Elliott and A. Novick-Cohen, *The Cahn-Hilliard equation with a concentration dependent mobility. Motion by minus the Laplacian of the mean curvature*, Euro. J. Appl. Math., 7, 287-301, 1996.

[6] C. M. Elliott and H. Garcke, *On the Cahn-Hilliard equation with degenerate mobility*, SIAM J. Math. Anal., 27(2), 404-423, 1996.

[7] C. M. Elliott and Z. Songmu, *On the Cahn-Hilliard equation*, Arch. Rational Mech. Anal., 96(4), 339-357, 1986.

[8] J. B. Greer, *An improvement of a recent Eulerian method for solving PDEs on general geometries*, J. Sci. Comput., to appear.

[9] J. B. Greer, A. L. Bertozzi and G. Sapiro, *Fourth order partial differential equations on general geometries*, J. Comput. Phys., 216(1), 216-246, 2006.

[10] D. Halpern, O. E. Jenson and J. B. Grotberg, *A theoretical study of surfactant and liquid delivery into the lung*, J. Appl. Physiology, 85, 333-352, 1998.

[11] M. Hofer and H. Pottmann, *Energy-minimizing splines in manifolds*, ACM Trans. Graphics, 23, 284-293, 2004.

[12] M. J. Holst, *Adaptive numerical treatment of elliptic systems on manifolds*, Adv. Comput. Math., 15, 139-191, 2001.

[13] M. J. Holst and D. Bernstein, *Adaptive finite element solution of the initial value problem in general relativity I: algorithms*, in preparation.

[14] F. Memoli and G. Sapiro, *Fast computation of weighted distance functions and geodesics on implicit hyper-surfaces*, J. Comput. Phys., 173(2), 730-764, 2001.

[15] F. Memoli, G. Sapiro and P. Thompson, *Implicit brain imaging*, Human Brain Mapping, 23, 179-188, 2004.

[16] T. G. Myers and J. P. F. Charpin, *A mathematical model for atmospheric ice accretion and water flow on a cold surface*, Int. J. Heat Mass Trans., 47, 5483-5500, 2004.

[17] S. Osher and R. Fedkiw, *Level Set Methods and Dynamic Implicit Sufaces*, Springer-Verlag, 2003.

[18] R. Pego, *Front migration in the nonlinear Cahn–Hilliard equation*, Proc. Roy. Soc. London Ser. A, 422, 261-278, 1989.

[19] A. Rätz, A. Ribalta and A. Voigt, *Surface evolution of elastically stressed films under deposition by a diffuse interface model*, J. Comput. Phys., 214(1), 187-208, 2006.

[20] A. Rätz and A. Voigt, *A diffuse interface approximation for surface diffusion including adatoms*, UCLA CAM report, 06-45, 2005.

[21] J. A. Sethian, *Level Set Methods and Hast Marching Method. Evolving Interfaces in Computational Geometry, Fluid Mechanics, Computer Vision, and Materials Sciences*, Cambridge University Press, 1999.

[22] S. Vey and A. Voigt, *AMDiS - Adaptive multidimensional simulations*, Comp. Vis. Sci., to appear.

[23] J. Xu and H. K. Zhao, *An Eulerian formulation for solving partial differential equations along a moving interface*, J. Sci. Comput., 19, 573-594, 2003.